Journal of Great Lakes Research Supplement 39 (2013) 183–193

Contents lists available at ScienceDirect

Journal of Great Lakes Research

journal homepage: www.elsevier.com/locate/jglr

High frequency radar and its application to fresh water

Lorelle A. Meadows [a,*], Chad Whelan [b,1], Don Barrick [b,1], Rachael Kroodsma [c,2], Christopher Ruf [c,2], Calvin C. Teague [b,1], Guy A. Meadows [c,2], Suwen Wang [b,1]

[a] College of Engineering, University of Michigan, 1261 Lurie Engineering Center, Ann Arbor, MI 48109-2102, USA
[b] CODAR Ocean Sensors, Ltd., 1914 Plymouth St # B Mountain View, CA 94043, USA
[c] Dept. of Atmospheric, Oceanic and Space Sciences, University of Michigan, 2455 Hayward St., Ann Arbor, MI 48109-2143, USA

ARTICLE INFO

Article history:
Received 28 December 2011
Accepted 8 June 2012
Available online 6 March 2013

Communicated by Robert Shuchman

Keywords:
Remote sensing
High frequency radar
Coastal processes
Instrumentation

ABSTRACT

High frequency (HF) radar has become an important tool for remotely mapping the spatial distribution and temporal evolution of waves and currents of the nearshore coastal ocean. Its acceptance along ocean coasts has resulted in the development of several commercially available systems and a planned nationwide coastal network to routinely measure coastal currents. Because HF radiation is known to propagate less efficiently over fresh water than seawater, it has been largely overlooked as a viable tool for freshwater application. However, its potential utility in freshwater was clearly demonstrated by a deployment along Lake Michigan as part of the 1999–2001 Episodic Events Great Lakes Experiment. As part of this experiment, the University of Michigan Multi-frequency Coastal Radar consistently produced reliable near surface current measurements to a range of approximately 25 km offshore showing strong correlation with both in-situ measurements and numerical hind-casts. This paper provides background on HF radar technology, a summary of the current state of the art with respect to freshwater and describes the results of a recent experiment to measure the propagation of HF radar signal over freshwater using CODAR Ocean Sensors SeaSondes, operating at 5 and 42 MHz with 21 W and 90 W average radiated powers, respectively. The effective offshore range for these radars was found to be 18 km at 5 MHz and 4–5 km at 42 MHz. These findings are consistent with currently available models for the prediction of propagation loss, verifying that they can reliably be used to estimate ranges in freshwater settings.

Introduction

The coherent backscatter of high frequency (HF) radar waves (10 to 100 m wavelengths) at grazing incidence from the ocean surface was first observed by Crombie (1955). He found that the peak in the backscattered Doppler spectrum was located approximately at the frequency of ocean surface gravity waves with wavelengths on the order of one half the radar wavelength. These findings indicated that radio waves reflected from the sea obey Bragg scattering in which the ocean surface acts as a diffraction grating. To first order, the strong HF echo arises from a Bragg scattering interaction with ocean waves traveling radially with respect to the radar and having a wavelength of one half the radar wavelength.

Observed Doppler spectra, as shown in Fig. 1, reveal the dominant, first order Bragg echo peaks as described by Barrick (1971) at a Doppler shift corresponding very nearly to the phase velocity of the radially advancing and receding waves. The Doppler shift, Δf, can be approximated by

$$\Delta f = (2fc)/c_{em}, \tag{1}$$

where f is the transmit frequency of the radar, c is the radial velocity of the Bragg resonant waves and c_{em} is the speed of light in free space and $c \ll c_{em}$. In the absence of an underlying current, these first order Bragg peaks, visible in Fig. 1 at $\Delta f \sim \pm 0.72$ Hz, correspond directly to the first order phase velocity of Bragg-resonant surface gravity waves traveling radially toward or away from the radar.

The presence of near-surface currents perturbs the phase speed of the surface gravity waves. Stewart and Joy (1974) estimate the influence of near surface currents U on wave phase speed via

$$c = c_p + \partial c(k) \tag{2}$$

in which

$$\partial c(k) = 2k \int_{-\infty}^{0} U(z) e^{2kz} dz. \tag{3}$$

* Corresponding author. Tel.: +1 734 764 2244.
E-mail addresses: lmeadows@umich.edu (L.A. Meadows), chad@codar.com (C. Whelan), don@codar.com (D. Barrick), rakro@umich.edu (R. Kroodsma), cruf@umich.edu (C. Ruf), cal@codar.com (C.C. Teague), gmeadows@umich.edu (G.A. Meadows), suwen@codar.com (S. Wang).
[1] Tel.: +1 408 773 8240.
[2] Tel.: +1 734 647 3660.

0380-1330/$ – see front matter
http://dx.doi.org/10.1016/j.jglr.2013.01.002

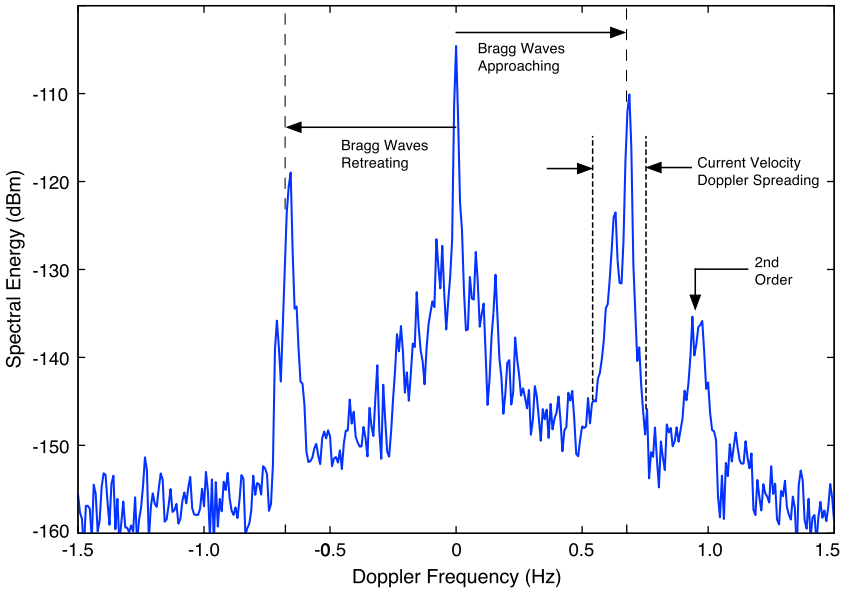

Fig. 1. Typical HF (high frequency) ocean surface Doppler spectrum at 25 MHz (Harlan et al., 2010) with first order Bragg peaks from surface waves that are half the radar wavelength traveling toward (positive Doppler) and away (negative Doppler) from the radar. A second order peak from longer waves modulating the Bragg wave is visible to the right.

Here, $U(z)$ is the horizontal current velocity profile as a function of depth z (negative downwards) and $U \ll c_p$. Given a measurement of c from the Doppler spectrum observation of Δf (Fig. 1), and knowing the theoretical wave phase speed, c_p, as derived from the dispersion relation for deep water gravity waves:

$$c_p = (g/k)^{1/2} \tag{4}$$

in which g is the acceleration due to gravity and k is the radar wavenumber, Eq. (2) yields a value for $\partial c(k)$. Stewart and Joy (1974) estimate that this value is approximately equivalent to the current at a depth of 4% of the Bragg resonant wavelength.

Since a single system is only able to retrieve the radial component of near surface current velocity, it is typical to pair systems and retrieve two different radial components over a footprint in order to construct the full vector field.

HF radar applications

In addition to surface currents, primary and secondary HF spectra have been used to determine surface wind speed and direction (Vesecky et al., 2005), track sea-going vessels and other hard targets (Fernandez et al., 2001), determine wave field characteristics (significant wave height, dominant wave period and direction), as well as wave spectra (Wyatt, 2011) and with limited success in tracking ice flows (Potter and Weingartner, 2010). These products have been used to inform such diverse and important applications as search and rescue operations, water quality monitoring, marine navigation, rip current prediction, harmful algal bloom forecasts, ecosystem and fisheries management, oil spill response and hydrodynamic modeling. Because of this significant utility for a broad scope of measurements and applications, HF radars have seen a ten-fold increase from 2004 to 2008, along with the development of a national network of HF systems for coastal surface current monitoring in the US ocean coasts (Harlan et al., 2009). Approximately 95% of HF radars operating in the U.S. are the compact cross-loop direction finding type. It is noteworthy that operational HF radar networks have to date been deployed exclusively for use over salt water with typical ranges of 15–20 km for VHF systems in the 42 MHz band up to 180–220 km for the lowest frequencies in the 5 MHz band. We consider here the impact on radar performance of operation over fresh water.

HF radar measurement range

The range over which any radar is capable of making measurements is a function of the signal-to-noise ratio (SNR) of the received signal scattered by its targets. In the case of HF radar for current mapping, the targets are the surface waves. The equation for determining the SNR for any target is given as:

$$SNR = P_T \frac{G_T D_R F^4 \lambda^2 \sigma_t \tau}{(4\pi)^3 R^4 k T F_a} \tag{5}$$

where P_T is the average radiated power, G_T the transmit antenna power gain, D_R the receive antenna directivity, λ the radar wavelength, τ the coherent FFT processing time, σ_t the radar cross section of water surface within the radar cell, R the range to the radar cell, kT the internal receiver thermal noise spectral density (4×10^{-21} W/Hz), F_a the factor by which external noise exceeds internal receiver noise, and F the normalized one-way field strength attenuation factor. The last parameter, F, is the only term in the expression for SNR that changes between freshwater and seawater. F depends on transmit frequency, water dielectric permittivity and conductivity, distance and surface roughness (sea state) and it includes the effects of diffraction over the spherical earth. The normalization is such that this factor is unity for a flat, perfectly conducting surface and/or at very short distances. Values of F for freshwater and seawater can be calculated accurately from GRWAVE, the program recommended by ITU/NATO and the accepted standard for 40 years (Rotheram, 1981). A comparison of freshwater to seawater range performance for three different frequencies is shown in Fig. 2. Typical values for transmit power, antenna gain and wave state account for the range of distances plotted on each curve. The difference in values between freshwater and seawater is primarily due to the difference in salinity, which primarily affects the conductivity.

To achieve range distances beyond the horizon, the electromagnetic signal must couple with the surface and propagate via groundwave mode. For typical ocean surface water with salinity over 30 ppt, the higher conductivity favors HF coupling to the sea surface and allows the signal to travel significantly farther than over land or freshwater.

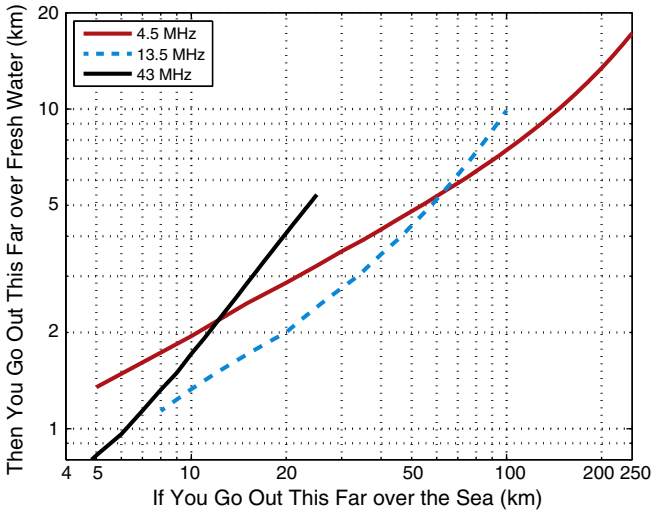

Fig. 2. Ratio of range achieved over seawater vs. freshwater assuming a common SNR (signal-to-noise ratio) at three transmission frequencies.

Lowering the salinity has been shown to significantly reduce the range performance of coastal ocean systems during periods of high freshwater discharge (Harlan et al., 2010). For this reason, HF radar has not generally been considered suitable for freshwater measurements. Additionally, lakes, even large lakes, often have limited fetch lengths, resulting in shorter wavelengths and less developed sea states than most ocean coasts. This can result in the lack of the presence of waves that are resonant with HF radar frequencies.

Despite the limitations of HF radar over freshwater, its potential utility was demonstrated by deployments of the University of Michigan Multi-frequency Coastal Radar (MCR), along Lake Michigan as part of the 1999–2001 Episodic Events Great Lakes Experiment (Fernandez et al., 2000; Meadows et al., 2000; Teague et al., 2000; Vesecky et al., 1999, 2000, 2001a, 2001b). During this experiment, the MCR, which could transmit and receive on four multiplexed frequencies, produced surface current measurements up to a range of approximately 25 km offshore with the lowest frequency of 4.8 MHz. These measurements showed strong correlation with both in-situ acoustic Doppler current measurements and numerical hind-casts of surface current conditions. Although fetch-limited wave growth theory indicates a stronger potential for the existence of Bragg scattering components in the Great Lakes setting at higher frequencies (above approximately 14 MHz), actual data return with the MCR over freshwater was much greater for lower frequencies. This is in part due to the increased natural power loss with propagation distance at higher frequencies. Successful retrieval out to 20 km for winds over the lake in excess of 3 m/s was repeatedly achieved at 4.8 MHz.

Factors related to improving range performance on freshwater that will not be addressed here are the transmit antenna power gain, G_T, and the receive antenna directivity, D_R. Transmit antenna power gain can be easily calculated based on the antenna design and most commercial HF radar systems available today can be configured with directional transmit antenna gain. For receive antennas, there are two basic types that are available on the market: compact direction finding and linear phased array. Compact systems consist of co-located directional antennas or a small footprint (2–9 m^2) array. The signals from two or more receive antennas are compared to determine the direction of arrival of the signal based on optimization techniques such as Least Squares or Multiple Signal Characterization (MUSIC) (Teague et al., 1997). Phased array systems consist of a relatively large linear array of antennas that can resolve direction either by forming a beam digitally with a width that is a function of array length (in radar wavelengths) or they may employ direction finding.

Methods

Measurement of HF propagation characteristics over freshwater

In Spring 2011, an experiment was conducted to measure the propagation characteristics of HF transmission over freshwater using a commercially available HF radar system operating at a range of frequencies. Specifically, the field deployment consisted of the installation and operation of two SeaSonde HF radar systems manufactured by CODAR Ocean Sensors. The radars operated at 42 MHz and 5.375 MHz, near the top and bottom of the range of frequencies currently used for ocean measurements in the U.S. A third custom-built directional receive antenna operating at 5.375 MHz was also deployed. The selection of these frequencies was designed to assess HF performance for both low frequency transmission, which has been shown to provide consistent results to 20 km range over freshwater in the presence of resonant surface waves, and high frequency transmission, for which fetch-limited wave growth theory suggests a higher likelihood for the existence of Bragg scattering components in the Great Lakes.

The 42 MHz SeaSonde system consisted of a single basic unit comprised of an omni-directional transmit/receive mast. The 5.375 MHz SeaSonde system consisted of an omni-directional transmit antenna and a separate directional receive antenna. Both units were installed as close as possible to the water surface, less than 10 meters away from the land/water interface, and approximately 1 meter above the still water level. Each receive mast consisted of three antennas: two directional loop antennas and an omnidirectional dipole. The pulse modulation waveform used is Frequency Modulated interrupted Continuous Wave (FMiCW) with an effective radiated power of 52 W. Processing of Doppler spectra was performed on site to provide radial current maps in near real time. In addition to the SeaSonde antennas, a custom built three-element end fire array tuned to 5.375 MHz was installed to test range improvement with increased antenna gain. Each array element consisted of a quarter-wave loop magnetic dipole antenna coupled to a small step down secondary loop. The secondaries were fed by 50 ohm coaxial cable phased to produce an end fire pattern perpendicular to the coastline with measured azimuthal half power beam width of 105 degrees and gain 5.1 dB above that of the commercial SeaSonde receive antenna. The narrower bandwidth of the end fire array made it suitable for the CW propagation tests but not the pulsed radar backscatter measurements, which were performed using the SeaSonde antenna.

Site selection for the deployment was based on an evaluation of the dominant environmental conditions over Lake Michigan for the deployment month of May. An evaluation of detailed hindcast wave data, available through the NOAA Great Lakes Coastal Forecasting System for Lake Michigan, was performed. Fig. 3 provides a summary evaluation of the wave climate along the Lake Michigan coastline of the State of Michigan. In May, the northern portion of Lake Michigan experiences a much higher likelihood of significant wave height in excess of 0.5 m; approximately twice as frequent as the southern end of Lake Michigan. Based on this analysis and the availability of property with access to the lake at low elevation, Point Betsie (lat 44.691° N, lon 86.255° W) was chosen as the deployment site.

Fig. 4 provides a site diagram showing the location of the field deployment site. The radar systems were set up on May 9 and antenna transmission was tested through the following day under relatively low wind and wave conditions. The systems were then operated nearly continuously from May 11 through May 19. On May 20, the systems were dismantled. Propagation measurements were made on May 12, 18 and 19 by setting the systems to transmit mode and measuring the received signal strength at various distances offshore. The SeaSonde systems were calibrated on May 11.

To complement and support the HF data acquisition, two additional data sources were employed. For in-situ instrumentation, an acoustic Doppler current profiler (ADCP) was deployed to collect wave and

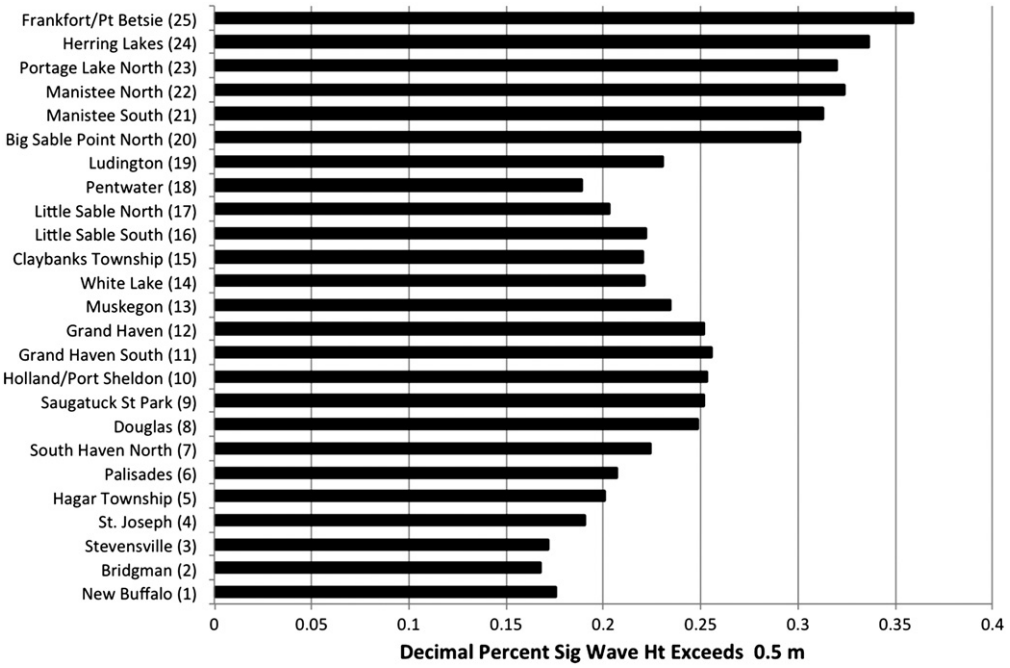

Fig. 3. Percent of time during the month of May that waves exceed 0.5 m significant wave height, averaged for 2006 through 2010, for 25 sites on the Lake Michigan shoreline. The northern portion of the lake exhibits higher occurrence of waves in excess of 0.5 m significant wave height. Based on Great Lakes Coastal Forecasting System hindcast estimates of wave conditions in Lake Michigan. Site locations are provided in Fig. 4.

near surface current measurements offshore of Point Betsie. Unfortunately, this instrument malfunctioned approximately 2 days into the deployment, collecting environmental data only during the setup period. A second source of environmental data was obtained via the hindcast model available through the Great Lakes Coastal Forecasting System of the National Oceanic and Atmospheric Administration Great Lakes Environmental Research Laboratory (http://www.glerl.noaa.gov/res/glcfs/). During the time period of the field deployment the National Data Buoy Center Northern Lake Michigan Buoy (45002) was not in place. Fig. 5 provides a time series overview of the model-reported environmental conditions in the vicinity of the ADCP deployment site.

Results and discussion

Propagation tests

Three transects were performed to measure the one-way propagation loss over fresh water. For each transect, the radar was set to continuous wave (CW) mode, generating a signal at a single frequency without the sweeping or pulsing that are necessary for processing Doppler-shifted echoes. The 42 MHz SeaSonde transmitted with an effective radiated power (ERP) of approximately 90 W. The Long Range SeaSonde transmitted with 21 W ERP when using the standard

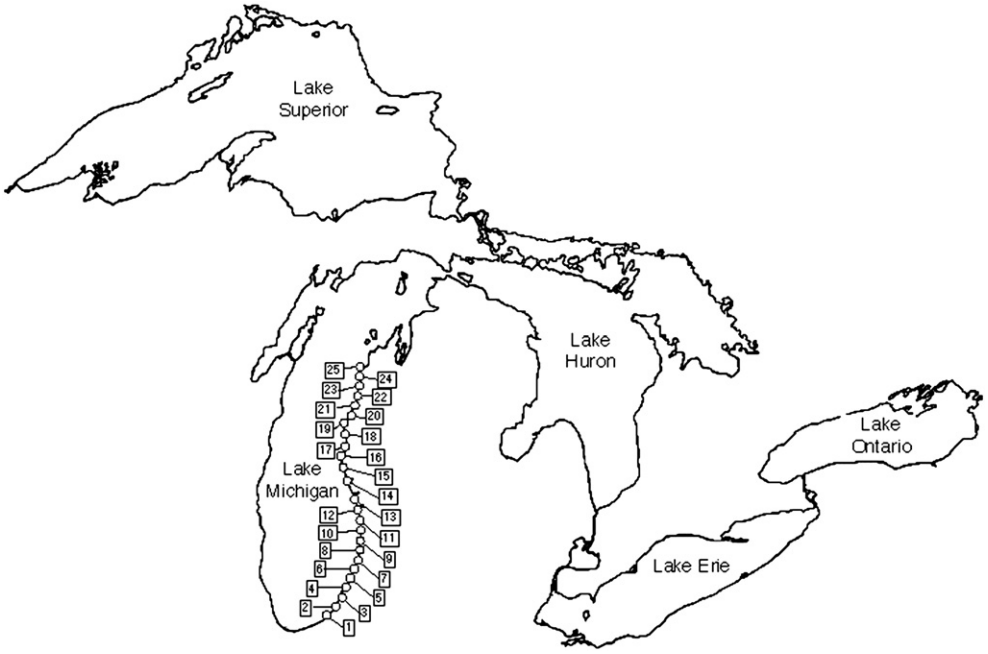

Fig. 4. Site map of the Great Lakes basin showing the positions of wave hindcast climate evaluation sites noted in Fig. 3. Site number 25 is the field experimental site, Point Betsie on Lake Michigan.

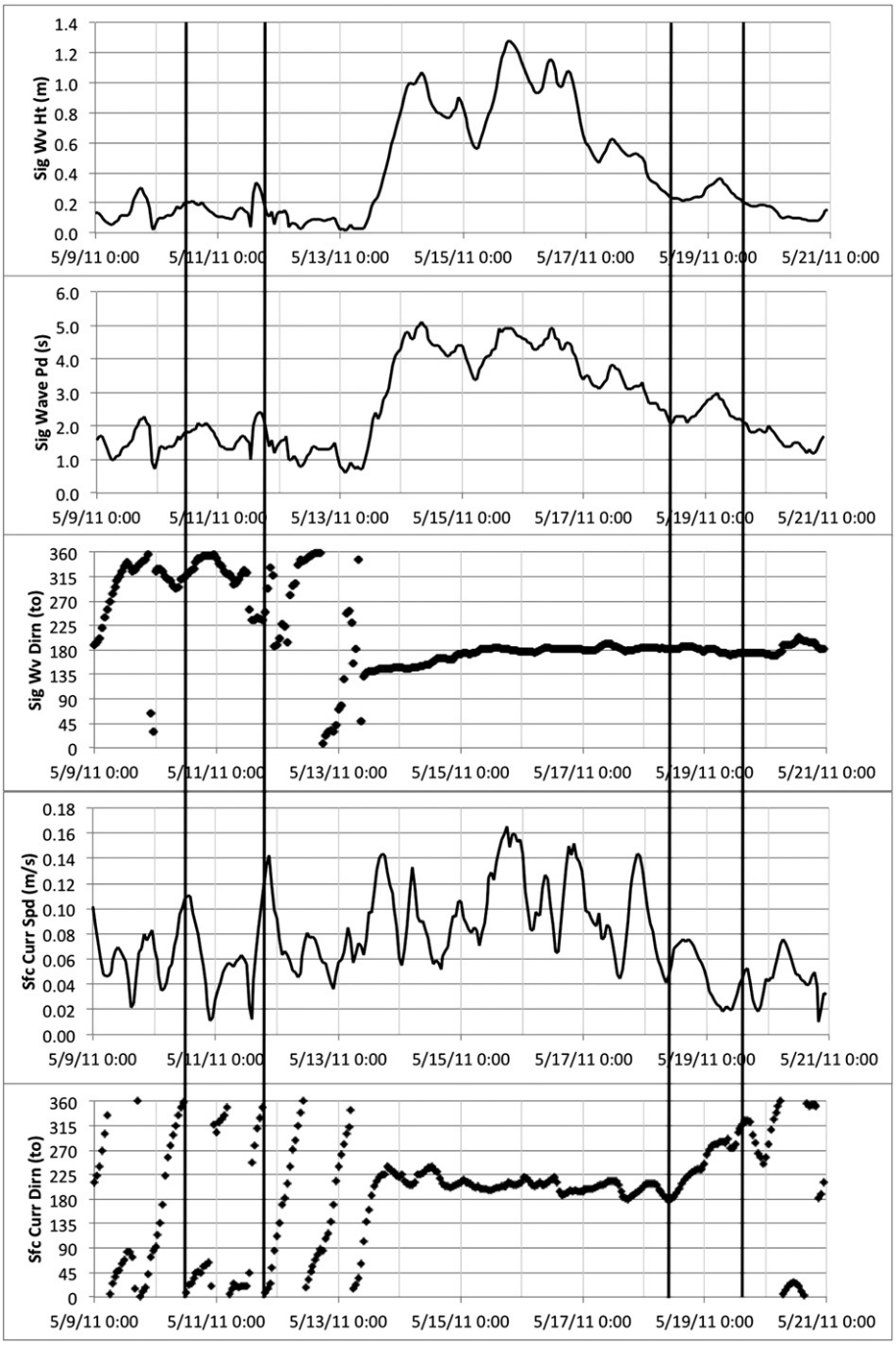

Fig. 5. Wave and current conditions at Point Betsie during the 2011 HF (High Frequency) Great Lakes Deployment as determined by the Great Lakes Coastal Forecasting System hindcast. Data includes significant wave height, period and direction as well as surface current speed and direction. Times in GMT. Directions indicate flow toward this direction. Vertical lines indicate approximate times of propagation test measurements.

SeaSonde omnidirectional monopole transmit antenna and 94 W ERP when connected to the University of Michigan (UM) directional transmit array. Measurements for the 42 MHz SeaSonde were made with the same settings for all three transects. For the 5 MHz band, one transect was completed using the UM transmit array and two transects were conducted using the SeaSonde transmit antenna. The waves in all transects were less than 0.2 m. In all cases the survey vessel conducted transects to and from shore along the bore sight of the radar antennas. These surveys were conducted to an offshore distance where the transmitted signal was lost in the background noise. This typically occurred at ranges of approximately 30–40 km. Hence, relatively low sea state conditions were required to complete the propagation tests.

A spectrum analyzer connected to a receive antenna on the boat was used to measure the radar signal for each transect. For the 5 MHz signal, the spectrum analyzer center frequency was set at 5.375 MHz with a span of 1 kHz and a resolution bandwidth (RBW) of 10 Hz (101 point FFT). For the 42 MHz radar, the spectrum analyzer center frequency was set at 42 MHz with a span of 1 kHz and a RBW of 10 Hz (101 point FFT). 100 sweeps were averaged in order to reduce the receiver

noise. First, the spectrum analyzer was connected to the antenna and the data file was saved that included the 100 averaged sweeps. A 50 ohm load was then connected to the spectrum analyzer and the 100 averaged sweeps was taken. To process the data, the peak power level was selected along with the value of the power of the load at that same frequency and the difference between the antenna and load was taken. This process was performed at a distance from shore of 1–8 lm at 1 km intervals, 8–16 km at 2 km intervals, and 16–32 km at 4 km intervals.

The results of these measurements are shown in Figs. 6 and 7 for 42 and 5 MHz, respectively. Measured transect data are plotted over theoretical propagation loss curves for freshwater and seawater. These curves were plotted using a derivative of GRWAVE (see Barrick, 1971), an ITU standard for calculating ground-wave propagation that allows effects of surface roughness to be included. Dielectric constant for both sea and fresh water is 81. The conductivity of sea water is 4 mhos/m, while that of fresh water was taken to be zero (the difference between results for zero and the normal range of freshwater conductivity is negligible). The effect of surface roughness on fresh water is negligible for the normal range of wave heights, although roughness effect on attenuation is significant over sea water at higher HF/VHF frequencies).

All predicted curves and measured data sets are individually normalized relative to their values at 1 km, the closest measurement range. Normalization is done to eliminate differences in transmit power levels, transmit antenna gains, receive antenna gain and spectrum analyzer gain. Daily differences of up to 1 dB are expected with different wave states and ground moisture levels between the antenna and water. Measurements made using the SeaSonde transmit antennas were all within ± 1 dB of each other on the respective frequencies. The increased transmit antenna gain with the UM antenna produced a 10 dB increase in received signal strength throughout all ranges. Figs. 6 and 7 illustrate that the rate of propagation loss at Point Betsie follows the freshwater curve and not the seawater curve. It should be noted that in order to compare the overall relative difference in performance between freshwater and seawater, the values plotted in Figs. 6 and 7 would need to be normalized at the coastline, rather than 1 km offshore. For 42 MHz, GRWAVE results indicate that propagation loss over the first kilometer

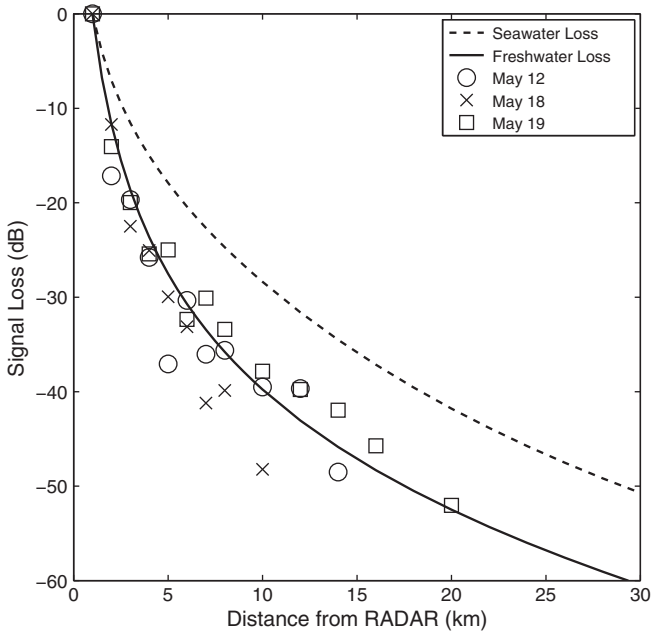

Fig. 6. One-way propagation loss for 42 MHz SeaSonde system. Data sets (symbols) and theoretical curves (solid lines) are all normalized individually relative to values measured or predicted at 1 km range.

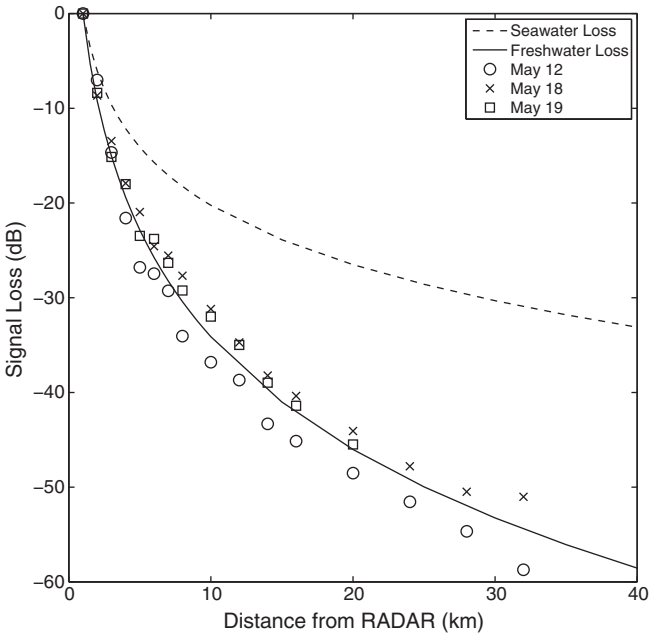

Fig. 7. One-way propagation loss for 5 MHz SeaSonde system. Data sets (symbols) and theoretical curves (solid lines) are all normalized individually relative to values measured or predicted at 1 km range.

for freshwater is predicted to be 8 dB more than for seawater. For the 5 MHz band, the GRWAVE predicted additional propagation loss is 20 dB over seawater.

Surface wave echoes

Except for the periods when the transects were performed, both the 42 MHz and 5 MHz SeaSondes were configured to collect and process Bragg echo from surface waves into a map of the polar projection of surface currents. The 5 MHz Bragg echo data were effectively only usable the last three days of the experiment, May 17–19, due to interference in the first few range cells caused by a ringing that occurred in the UM array. The ringing resulted from resonant excitation of the UM antenna by the transmitted signal, which took ~200 μs to decay due to the high (~500) Q of the magnetic diploes. It was initially identified by noting that the DC signal, which usually results from echoes from stationary targets, was much stronger than normally observed and had an exponential time decay (over several time constants) which is characteristic of a high-Q tuned circuit but not land echoes (Teague, personal communication, 2011). Once this ringing was discovered, the UM array was disabled during data collect on the 5 MHz SeaSonde system.

An example of a 5 MHz SeaSonde Doppler spectrum from Lake Michigan is shown in Fig. 8. The thin peak at 0 Hz (middle of the plot) is echo from stationary objects that do not produce Doppler frequency shift (buildings, land, etc.) as well other energy in the system that is mixed down to 0 Hz in Doppler processing. The Bragg echo due to waves of half the radar wavelength traveling toward and away from the radar can be seen in the thin peaks on the positive (right) and negative (left) of 0 Hz, respectively. The Bragg energy on the positive side, from waves moving toward the shore, was always stronger in this experiment so it was used as the measure of range performance of the system. Signals reported here were recorded on the omnidirectional 3 dBi gain receive dipole.

Fig. 9 shows the 42 MHz SeaSonde SNR during wave states when significant wave height as produced by hindcast model varied between 0.6 and 1.0 m on May 14 & 15. Individual measurements are plotted as hollow circles with the mean values plotted as the solid curve. The standard SeaSonde cutoff of 6 dB is plotted as a solid horizontal line and the effective range is 7–8 km. Low SNR in range cells below 2 km are due to

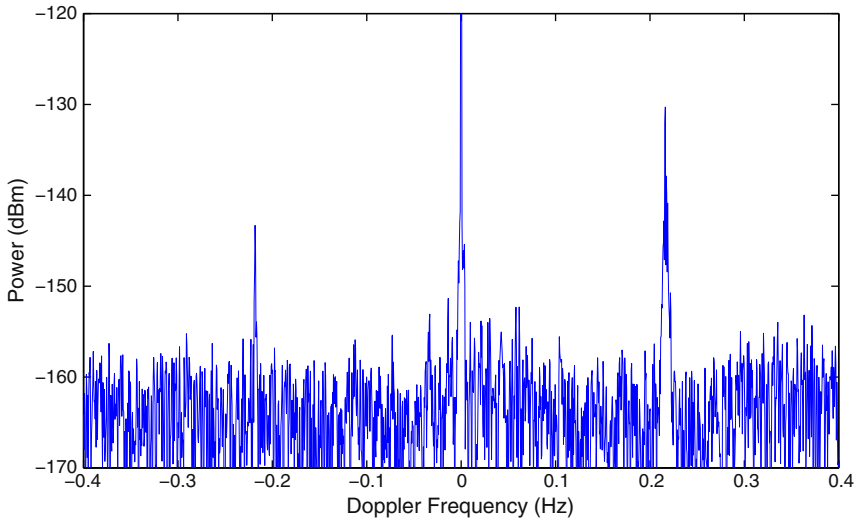

Fig. 8. An example of a 5 MHz Doppler spectra from a SeaSonde system obtained at a location approximately 6 km offshore of Point Betsie. Spectral lines at ±0.23 Hz on the x-axis are echoes from lake waves moving radially toward and away from the radar. The line at zero Doppler (zero on the x-axis) is due to echoes from stationary objects or received response.

improper setting of transmit blank delay, which is the time delay following a transmit pulse before the system begins receiving echoes. This is normally set to 8.55 μs for long range systems such that no echoes are received from ranges less than 1.28 km. Since long range HF radars typically have range resolutions of 3–10 km, depending on frequency bandwidth, this is well below the range resolution. For higher resolution systems, transmit blank delay should be set lower.

The radial distribution for 42 MHz SeaSonde on May 14 & 15, when significant wave height varied between 0.6 and 1.0 m, is shown in Fig. 10. The gray scale is a measure of the percentage of time a vector solution is found at a given range and bearing with darker grays indicating a higher percentage of returns. Radial solutions are consistently found out to 4–5 km. Azimuthal gaps are due to antenna interactions with near field environment. The 42 MHz antenna was installed in the vicinity of a metal-sided building. Although more than one wavelength from the antenna, the corrugated sheet metal wall of the building could have degraded the antenna pattern significantly.

Fig. 11 shows the 42 MHz SeaSonde SNR during a period of time when the hindcast significant wave height varied between 0.2 and 0.4 m on May 19. This period of increasing wave height was coincident with a shift in wind direction to the north and an associated increase in wind speed above 3 m/s with sustained winds above approximately 5 m/s. Individual measurements are plotted as hollow circles with the mean values plotted as a solid curve. The standard SeaSonde minimum SNR threshold of 6 dB is plotted as a horizontal line and the effective range is 4–5 km. The radial distribution for this period is shown in Fig. 12. The range of radial solutions matches the effective range determined by signal strength, as expected. Additionally, the distribution was more sparse in bearing at the lower wave state, possibly due to weaker wind-driven currents that defy the detectability limits of the system.

To provide better load matching for the long range SeaSonde transmit antenna, 4.57 MHz was used for the surface wave echo measurements. This also reduced the coupling to the UM antenna array. The amount of data collected at 5 MHz was limited to only a few days, so we do not have the same variety of wave states to compare range performance. In addition, operation at 5 MHz has the added challenge of fluctuating external background radio noise. This is primarily due to diurnal ionospheric variations which make 5 MHz skywave propagation more favorable in the evening when the D-layer absorption is low. This allows radio noise from man made and natural sources, like lightning storms, to travel much farther. At Point Betsie, the background RF (radio frequency)

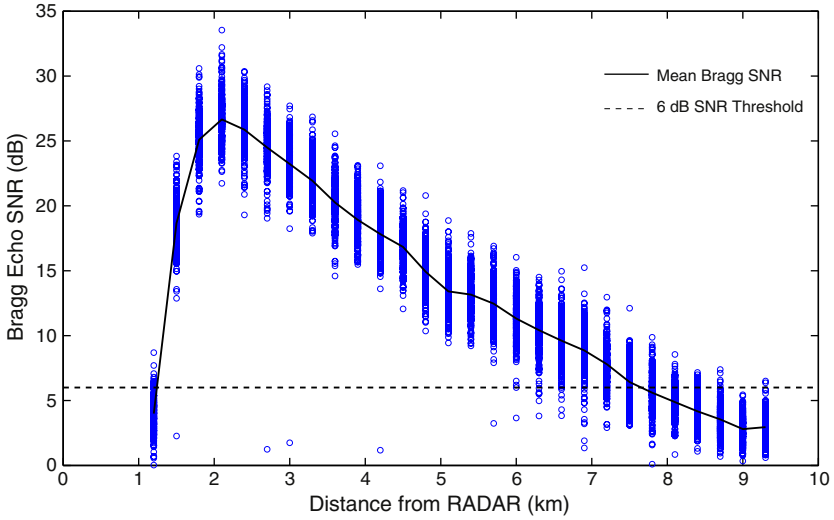

Fig. 9. Surface echo SNR (signal-to-noise ratio) vs. range for 42 MHz SeaSonde system on May 14 & 15 corresponding to significant wave heights of 0.6 to 1.0 m.

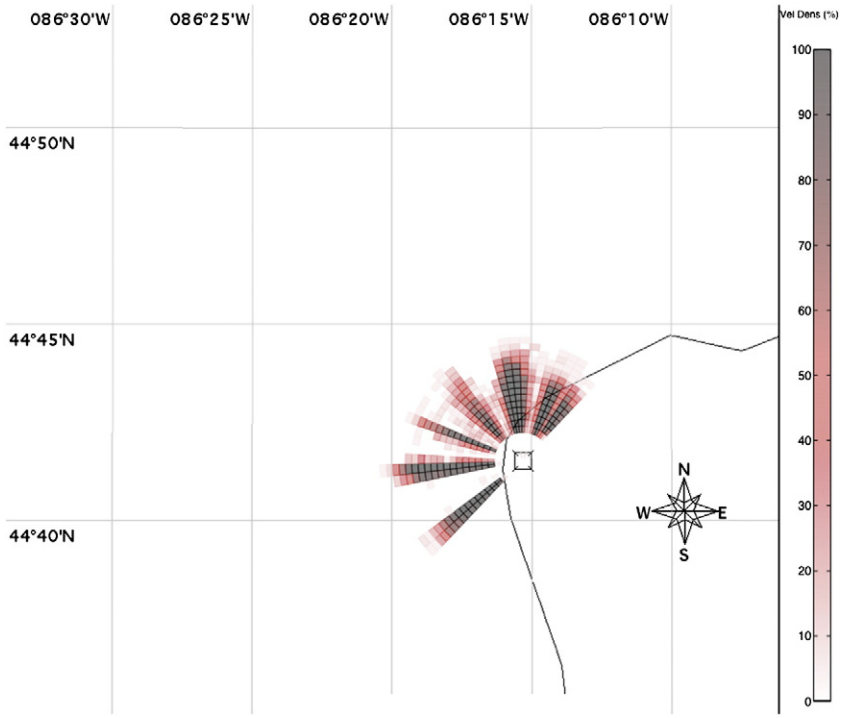

Fig. 10. Distribution of radial velocity measurement density (vel density) based on percentage of all retrieved radial measurements for 42 MHz SeaSonde system on May 14 & 15 corresponding to significant wave heights of 0.6 to 1.0 m.

noise level at 4.57 MHz increased approximately 10 dB, typically from approximately −163 dBm to −153 dBm, from day to evening as shown in Fig. 13. The 42 MHz system did not experience any noticeable diurnal variations of the background noise. Random fluctuations of the background noise at 42 MHz were in the 1–2 dB range.

Fig. 14 shows the 5 MHz SeaSonde SNR during wave states with significant wave height varying between 0.2 and 0.5 m during May 17–19. Individual measurements are plotted as hollow circles. Solid curves are six-hour means around 20:00 GMT (low external noise) on May 17 and 18, and around 06:00 GMT (high external noise) on May 8 and 19. Effective range during low noise period is 18 km vs. 9 km or less during high noise periods. The external noise, in this case, has a greater effect on range than does the wave state.

It should be noted that the radio bandwidth required to achieve the 3 km resolution is 50 kHz. Bandwidth this wide has been approved in other countries (e.g. Australia), but approval in the U.S. at 5 MHz is for specific scientific deployments only. Operational systems are limited to 25 kHz bandwidth, resulting in 6 km range resolution. Radial distribution for the long range system is shown in Fig. 15.

Conclusions

Range performance on freshwater is highly dependent on the presence of surface waves that are resonant with the radar frequency. At 42 MHz, the effective range for retrieval of currents varied between 4 and 8 km, depending on wave state, which varied between 0.2 and

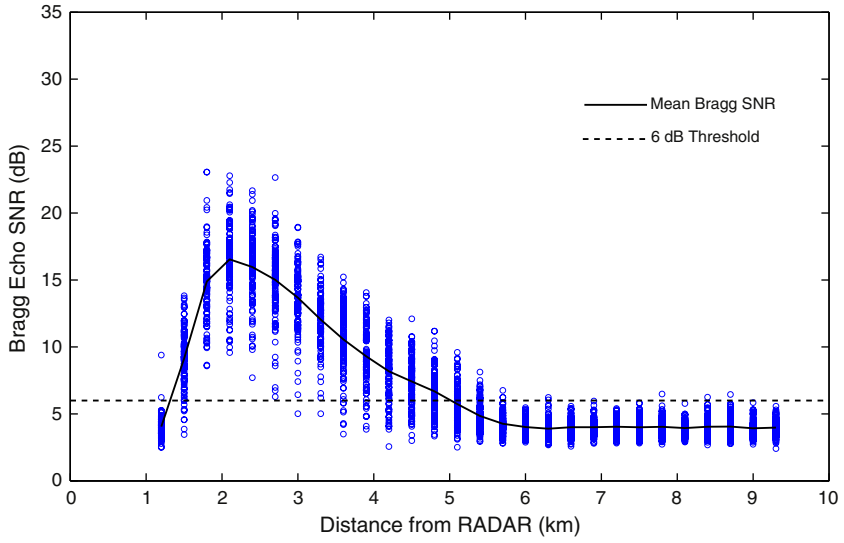

Fig. 11. Surface echo SNR (signal-to-noise ratio) vs. range for 42 MHz SeaSonde system on May 19 corresponding to significant wave heights of 0.2 to 0.4 m.

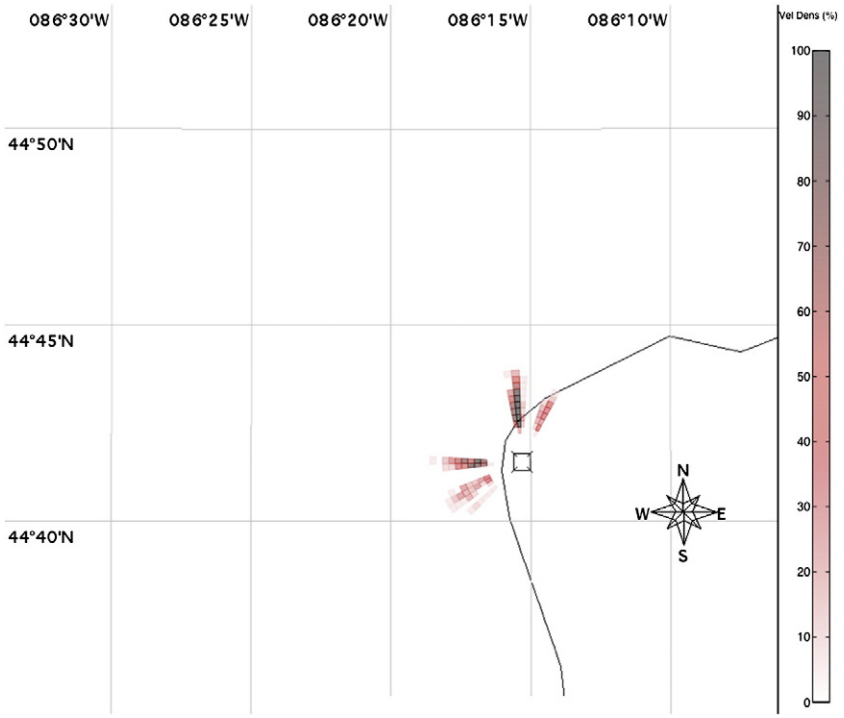

Fig. 12. Distribution of radial velocity measurement density (vel density) based on percentage of all retrieved radial measurements for 42 MHz SeaSonde system on May 19 corresponding to significant wave heights of 0.2 to 0.4 m.

1.0 m significant wave height. During periods of lower energy (waves and currents), azimuthal gaps that existed due to near-field antenna interactions were enhanced. Through careful deployment site selection, this interaction can be minimized leading to better azimuthal coverage in all conditions. At the highest wave heights, some second order Doppler spectra were visible that can be used for determining wave parameters. This could be investigated further. In a freshwater setting, a system of this frequency would have utility in the measurement of smaller scale flow structures very close to shore. In the Great Lakes, numerical modeling of the basin is limited by our poor understanding of the detailed physics of the coastal boundary layer. A system operating at 42 MHz could provide important insights to this gap in our knowledge.

Although limited to only a few days of the entire deployment, operation in the 5 MHz band had effective ranges between 3 and 18 km when significant wave height varied between 0.2 and 0.5 m. In addition to low wave conditions, effective range at 5 MHz was further limited by diurnal external background RF noise oscillations of 10 dB which resulted in a range reduction of 6–9 km. No second order Doppler spectra were visible during this period. Wave heights greater than 0.5 m occur approximately 35% of the time at Point Betsie based on the multi-season average, and less frequently at other locations. Coupled with the diurnal noise variation in the 5 MHz band, ranges of 18 km or greater are predicted to be achieved approximately 20% of the time for a standard SeaSonde configuration. This result is comparable to the results obtained by the previous, freshwater MCR experiment, described above (1999–2001). Although continuous operation in all sea state conditions is generally not possible, for some targeted applications, such as search and rescue, it is during higher wind and wave events that data on currents can play a critical role in mission success, especially in regions of complex topography and similarly complex current patterns. It is in these particular conditions that HF radar performs best.

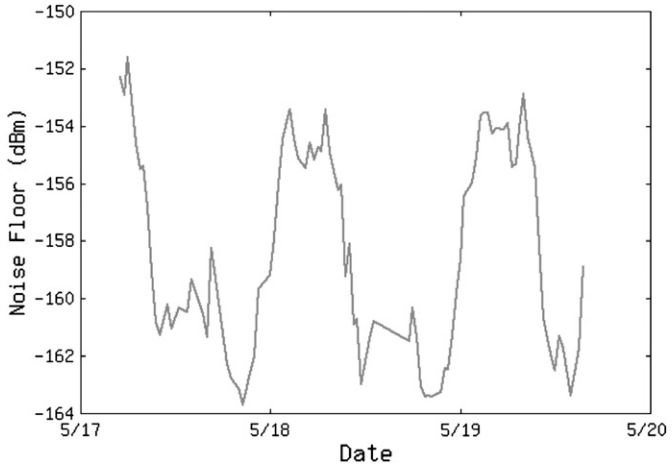

Fig. 13. Diurnal 10 dB (decibel) variation in external noise level observed at 4.57 MHz around Point Betsie. Time is in GMT.

Increased power and directional antenna gain do increase range, as demonstrated by the directional transmit antenna during the propagation tests. 10 dB gain in the bore sight direction was achieved due to both increased input power (possible with an improved impedance match) and higher directional gain. This amounts to approximately 6–9 km of additional range. As with any tuned antenna, care needs to be taken to ensure the proper bandwidth is available for the range resolution required.

Ultimately, the propagation tests indicate that the currently available models for theoretical predictions of propagation loss can be used to estimate ranges in fresh water and may be used to develop future enhancements to this technology for application in freshwater settings. Results of the overall experiment suggest that these enhancements should focus on the application of HF systems to specific target areas of high importance rather than a large-scale operational system for overall surface current mapping.

A recent report commissioned by the Great Lakes Environmental Research Laboratory (LimnoTech et al., 2011) identifies nine primary categories of user needs that should be addressed in the development of the Great Lakes Observing System. Among these are several applications where HF radar may play a role in critical data acquisition. These include improving the safety and efficiency of maritime operations

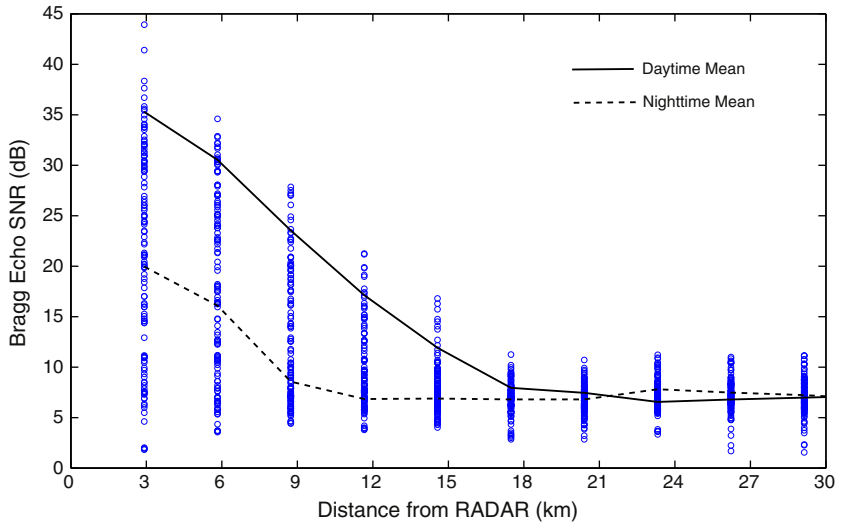

Fig. 14. Surface echo SNR (signal-to-noise ratio) vs. range for 5 MHz SeaSonde system during propagation test measurements conducted on May 17–19 (see Fig. 5 for approximate times and environmental conditions) corresponding to significant wave heights of 0.2 to 0.6 m.

through remote monitoring of operations in critical channels and harbors, improvement of nearshore health and minimization of public health risks through monitoring of physical processes associated with suspended and dissolved load transport on site-specific bases, and improved homeland security through measurement of parameters critical to local and renewable power sources and generation. Additional appropriate applications for HF radar in freshwater consist of monitoring of episodic events in support of increased understanding of the complex nearshore and coastal processes. Examples include rip current dynamics and conditions leading to beach closure events. It should also be noted that an operational HF radar system with Great Lakes range capability to 25 km from shore would capture the vast majority of commercial and private vessel traffic, cover all municipal water intakes, monitor most critical international borders and cover the extent of ice growth for most winters.

Acknowledgments

The authors wish to extend their thanks to the Friends of Point Betsie Lighthouse who provided site access and support for the field deployment. Over-water operations were managed aboard the University of Michigan Survey Vessel, Blue Traveler. This work was funded by a grant from the National Oceanic and Atmospheric Administration. Funding was also supplied from the International Ocean Observing System

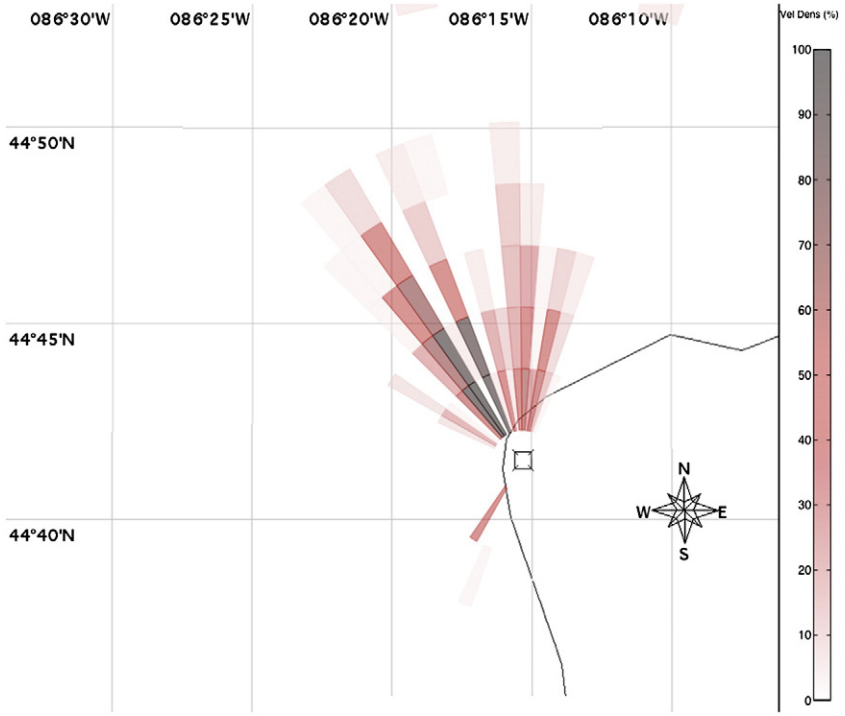

Fig. 15. Distribution of radial velocity measurement density (vel density) based on percentage of all retrieved radial measurements for 5 MHz SeaSonde system on May 17–19 corresponding to significant wave heights of 0.2 to 0.6 m.

program, via the Great Lakes Observing System, for support of the CODAR deployment.

References

Barrick, D.E., 1971. Theory of HF/VHF propagation across the rough sea. Part I: the effective surface impedance for a slightly rough highly conducting medium at grazing incidence. Radio Sci. 6, 517–526.

Crombie, D.D., 1955. Doppler spectrum of sea echo at 13.56 Mc/s. Nature 175, 681–682.

Fernandez, D., Meadows, L., Vesecky, J., Teague, C., Paduan, J., Hansen, P., 2000. Surface current measurements by HF radar in fresh water lakes. IEEE J. Ocean. Eng. 25 (4), 458–471.

Fernandez, D.M., Vesecky, J.F., Barrick, D.E., Teague, C.C., Plume, M.M., Whelan, C., 2001. Detection of ships with multi-frequency and CODAR SeaSonde HF radar systems. Can. J. Remote. Sens. 27 (4), 277–290.

Harlan, J., Terrill, E., Burnett, B., 2009. National high frequency radar network: update. Proc. of Oceans 2009. Marine Technology Society/Institute of Electrical and Electronics Engineers, pp. 1–7.

Harlan, J., Terrill, E., Hazard, L., Keen, C., Barrick, D., Whelan, C., Howden, S., Kohut, J., 2010. The integrated ocean observing system high-frequency radar network: status and local, regional, and national applications. Mar. Technol. Soc. J. 44, 122–132.

LimnoTech, Applied Science Associates, Clarkson University, Michigan Tech Research Institute, University of Minnesota — Duluth, 2011. DESIGN REPORT Near-Term Design of the Great Lakes Observing System Enterprise Architecture, Prepared for: NOAA-GLERL Contract Number: WC133R-10-CN-0350, Ann Arbor, MI (82 pp.).

Meadows, L., Vesecky, J., Teague, C., Fernandez, Y., Meadows, G., 2000. Multi-frequency HF radar observations of the thermal front in the great lakes. Proceedings of International Geoscience and Remote Sensing Symposium. Institute of Electrical and Electronics Engineers, pp. 114–116.

Potter, R.A., Weingartner, T.J., 2010. Surface circulation radar mapping in Alaskan coastal waters: Beaufort Sea and cook inlet, final report. Outer Continental Shelf (OCS) Study Mineral Management Service (MMS) 2009-049.University of Alaska, Fairbanks (144 pp.).

Rotheram, S., 1981. Ground-wave propagation. Part 1: theory for short distances. Communications, Radar and Signal Processing: Institute of Electrical and Electronics Engineers Proceedings, 128(5), pp. 275–284.

Stewart, R.H., Joy, J.W., 1974. HF radio measurements of surface currents. Deep-Sea Res. 21, 1039–1049.

Teague, C.C., Vesecky, J.F., Fernandez, D.M., 1997. HF radar instruments, past to present. Oceanography 10 (2), 40–44.

Teague, C., Meadows, L., Vesecky, J., Fernandez, Y., Fernandez, D., 2000. HF radar observations of surface currents on Lake Michigan during episodic events great lakes experiment (EEGLE) 1999. Proceedings of International Geoscience and Remote Sensing Symposium. Institute of Electrical and Electronics Engineers, pp. 2949–2951.

Vesecky, J., Meadows, L., Daida, J., Hansen, P., Teague, C., Fernandez, D., Paduan, J., 1999. Surface current measurements by HF radar over fresh water at Lake Michigan and Lake Tahoe. Proceedings of Institute of Electrical and Electronics Engineers — Current Measurement Technology Conference, pp. 33–37.

Vesecky, J., Meadows, L., Teague, C., Fernandez, Y., Fernandez, D., Meadows, G., 2000. HF radar measurements of surface currents in fresh water: theoretical considerations and observational results. Proceedings of International Geoscience and Remote Sensing Symposium. Institute of Electrical and Electronics Engineers, pp. 117–119.

Vesecky, J., Meadows, L., Teague, C., Hansen, P., Plume, M., Fernandez, Y., 2001a. Surface current observations by HF radar during episodic events great lakes experiment (EEGLE) 2000. Proceedings of International Geoscience and Remote Sensing Symposium. Institute of Electrical and Electronics Engineers, pp. 272–274.

Vesecky, J., Drake, J., Plume, M., Meadows, L., Fernandez, Y., Hansen, P., Teague, C., Davidson, K., Paduan, J., 2001b. Multifrequency HF radar observations of surface currents: measurements from different systems and environments. Proceedings of Oceans. Institute of Electrical and Electronics Engineers, pp. 842–948.

Vesecky, J.F., Drake, J., Laws, K., Ludwig, F.L., Teague, C.C., Paduan, J., Meadows, L., 2005. Using multifrequency HF radar to estimate ocean wind fields. Proc. International Geoscience and Remote Sensing Symposium. Institute of Electrical and Electronics Engineers, pp. 1167–1170.

Wyatt, L., 2011. Wave mapping with HF radar, current, waves and turbulence measurements (CWTM). 2011 Institute of Electrical and Electronics Engineers/Oceanic Engineering Society 10th, pp. 25–30.